THE JOURNAL OF BIOLOGICAL CHEMISTRY
Vol. 277, No. 44, Issue of November 1, pp. 41948–41953, 2002
Printed in U.S.A.

Infectivity-associated Changes in the Transcriptional Repertoire of the Malaria Parasite Sporozoite Stage*

Received for publication, July 20, 2002, and in revised form, August 9, 2002
Published, JBC Papers in Press, August 12, 2002, DOI 10.1074/jbc.M207315200

Kai Matuschewski‡§¶, Jessica Ross‡, Stuart M. Brown‖, Karine Kaiser‡, Victor Nussenzweig‡, and Stefan H. I. Kappe‡

From the ‡Michael Heidelberger Division, Department of Pathology, New York University School of Medicine, New York, New York 10016, ‖Research Computing Resource, New York University Medical Center, New York, New York 10016, and §Department of Parasitology, Heidelberg University School of Medicine, 69120 Heidelberg, Germany

Injection of *Plasmodium* salivary gland sporozoites into the vertebrate host by *Anopheles* mosquitoes initiates malaria infection. Sporozoites develop within oocysts in the mosquito midgut and then enter and mature in the salivary glands. Although morphologically similar, oocyst sporozoites and salivary gland sporozoites differ strikingly in their infectivity to the mammalian host, ability to elicit protective immune responses, and cell motility. Here, we show that differential gene expression coincides with these dramatic phenotypic differences. Using suppression subtractive cDNA hybridization we identified highly up-regulated mRNAs transcribed from 30 distinct genes in salivary gland sporozoites. Of those genes, 29 are not significantly expressed in the parasite's blood stages. The most frequently recovered transcript encodes a protein kinase. Developmental up-regulation of specific mRNAs in the infectious transmission stage of *Plasmodium* indicates that their translation products may have unique roles in hepatocyte infection and/or development of liver stages.

Malaria transmission occurs by mosquito bite when *Plasmodium* sporozoites located in the salivary glands of anopheline mosquitoes enter the vertebrate host. Sporozoites invade hepatocytes and differentiate into exo-erythrocytic forms (EEFs)[1] that after a few days contain several thousand merozoites. After exiting the hepatocyte, merozoites invade erythrocytes and start the blood stage cycle that causes malaria disease. Salivary gland sporozoites and EEFs are rational targets for immunoprophylaxis and drug prophylaxis because they precede the development of the pathogenic blood stages. One important limitation for drug discovery and vaccine development is the lack of candidate target molecules specifically expressed in the pre-erythrocytic stages.

To date, only a few sporozoite-expressed proteins have been identified, mainly due to the difficulty of obtaining sporozoites in large quantities. Of those proteins, the sporozoite-specific coat protein CS (1, 2) and the sporozoite-specific invasin TRAP (3, 4) have been identified in a range of different *Plasmodium* species, and both proteins are lead malaria vaccine candidates either in single formulations or as components of multi-subunit vaccines (5, 6).

Sporozoite biology provides a unique opportunity to identify candidate virulence factors that contribute to the successful transmission of *Plasmodium*. We refer to the observations that oocyst sporozoites and salivary gland sporozoites display dramatically different phenotypes. Sporozoites isolated from the mosquito salivary glands are highly infectious to the mammalian host, migrate in a typical circular gliding pattern, and can elicit strong protective immune responses (7–10). In marked contrast, oocyst sporozoites are ~10,000-fold less infective to the mammalian host, do not exhibit circular gliding, and fail to produce protective immunity (Fig. 1). Furthermore, sporozoites that entered the salivary glands are no longer capable of reentering them, suggesting that the mature sporozoites are irreversibly programmed to invade mammalian hepatocytes and continue the life cycle (11).

We demonstrated previously that despite the technical challenges, basic transcriptional profiling of *Plasmodium* sporozoites using expressed sequence tag analysis is feasible (12). Here we investigated whether analysis of transcriptional differences between noninfective and infective sporozoites provides a means to efficiently identify genes controlling infectivity to the mammalian host. Using a suppression subtractive hybridization screen (13), we identify a number of developmentally up-regulated genes, demonstrating for the first time differential gene expression in sporozoites. The change in transcriptional repertoire could be an important mechanism controlling sporozoite infectivity and therefore transmission success.

EXPERIMENTAL PROCEDURES

Plasmodium berghei Life Cycle—Anopheles stephensi mosquitoes were raised at 28 °C, 75% humidity under a 14-h light/10-h dark cycle and maintained on a 10% sucrose solution during adult stages. 4–5-day-old female mosquitoes were blood-fed on anesthetized young S/D rats or Syrian hamsters that had been infected with the *P. berghei* strain NK65. Rodents were assayed for high levels of parasitemia and the abundance of gametocyte-stage parasites capable of exflagellation. After the infective blood meal, mosquitoes were maintained at 21 °C, 80% humidity. On day 10 postfeeding, mosquitoes were dissected in RPMI 1640 medium, and isolated midguts were examined for the infection rate. Only mosquito cages having at least 70% of mosquitoes infected were kept for further analysis. Sporozoite populations were separated as described previously (9, 10). Naive rodents were subjected to blood feeding of infected mosquitoes at day 18 postfeeding to maintain a continuous *P. berghei* cycle.

Generation of Subtraction Libraries—We dissected four million

* This work was supported by grants from the Deutsche Forschungsgemeinschaft (to K. M.) and National Institutes of Health (to V. N.) and a B. Levine fellowship in malaria vaccinology (to S. H. I. K.). The costs of publication of this article were defrayed in part by the payment of page charges. This article must therefore be hereby marked "*advertisement*" in accordance with 18 U.S.C. Section 1734 solely to indicate this fact.

¶ To whom correspondence should be addressed: Dept. of Parasitology, Heidelberg University School of Medicine, Im Neuenheimer Feld 324, 69120 Heidelberg, Germany. Tel.: 49-6221-565010; Fax: 49-6221-564643; E-mail: Kai_Matuschewski@med.uni-heidelberg.de.

[1] The abbreviations used are: EEF, exo-erythrocytic form; CS, circumsporozoite protein; MCP-1, merozoite capping protein-1; ORF, open reading frame; QRRT-PCR, quantitative real-time reverse transcription-PCR; RT-PCR, reverse transcription-PCR; TRAP, thrombospondin-related anonymous protein.

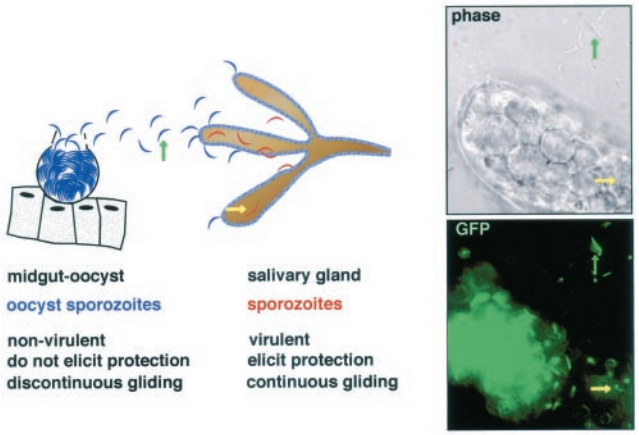

FIG. 1. **Localization of *Plasmodium* sporozoite populations within different organs of the mosquito vector coincides with different behavioral phenotypes.** Sporozoites are released from an oocyst that lodges between the mosquito midgut epithelium and the basal lamina. They reach the salivary gland by traveling through the mosquito hemocoel (*e.g.* sporozoite marked by *green arrow*). These sporozoites penetrate the salivary gland cells and migrate through and come to a rest in the lumen of the salivary gland duct (*e.g.* sporozoites marked by *yellow arrow*). At this stage, the sporozoites are ready for transmission through mosquito bite. The *right panels* show the median lobe of the mosquito salivary gland infected with sporozoites expressing the green fluorescent protein (30). In the *top right panel* (phase-contrast image), the extracellular sporozoites are clearly visible. In the *bottom right panel* (fluorescence image), extracellular sporozoites and sporozoites within the lobe are visualized.

P. berghei sporozoites each from midguts and salivary glands of infected *A. stephensi* mosquitoes. Salivary gland and oocyst sporozoites were purified over a DEAE-cellulose column to remove contaminating mosquito tissue. This crucial step resulted in one million highly purified parasites for each population. Poly(A)$^+$ RNA was isolated from these sporozoites, from 50 uninfected salivary glands, and from whole uninfected mosquitoes using oligo(dT) columns (Invitrogen). The poly(A)$^+$ RNA was used as a template for first-strand cDNA synthesis and one subsequent round of amplification using the SMART PCR cDNA synthesis kit (Clontech). Suppression subtractive hybridization was performed with the PCR-Select cDNA subtraction kit (Clontech). The subtracted cDNA population was ligated into vector pCR2.1-Topo (Invitrogen) and transformed into *Escherichia coli* TOP10 competent cells (Invitrogen). Sequencing was done at a DNA sequencing facility (Rockefeller University) by BigDye terminator cycle sequencing with the M13 reverse primer.

Sequence Analysis—The single-pass cDNA sequences from the subtraction libraries tended to be short and contained sequencing errors. It was possible to obtain some homology information by using the *P. berghei* cDNA sequences directly for BlastX searches against the GenBank™ nonredundant protein data base and the PlasmoDB automated predictions of *P. falciparum* proteins (PlasmoDB.org). However, more detailed information could be obtained by using the nearly complete genome sequence of the sibling species *P. yoelii* as a stepping stone (www.tigr.org). This enabled us to identify open reading frames (ORFs) and create predicted protein sequences for each gene. First the *P. berghei* cDNAs were clustered using the program Sequencher v3.1.1. The consensus sequences of clusters containing two or more *P. berghei* cDNA sequences were compared by BlastN to the PlasmoDB set of *P. yoelii* genomic contigs, and the single best matching contig was selected (>95% identity). The largest complete ORF was identified within the contig that overlapped the region matched by the cDNAs using the NCBI ORF Finder (www.ncbi.nlm.nih.gov/gorf).

The protein translation of each ORF was then used for a BlastP search of the GenBank™ nonredundant protein data base. We verified these ORFs by also using the entire sequence of the selected *P. yoelii* contigs for BlastX searches of the GenBank™ nonredundant protein data base. In every case, the ORF that overlapped the cDNA corresponded to the same region and reading frame of the contig as the best BlastX match for that contig. Functional predictions for putative *UIS* (up-regulated in infective sporozoites) genes were obtained by using the translated protein sequence of each ORF for hidden Markov models searches of the Pfam data base (pfam.wustl.edu/). Signal peptide predictions were done with SignalP (www.cbs.dtu.dk/services/SignalP), and prediction of transmembrane domains was done with Tmpred (www.ch.embnet.org/software/TMPRED_form.html).

Gene Expression Analysis—For mRNA expression analysis, we generated cDNA populations from around 50 ng of poly(A)$^+$ RNA obtained from 1 million purified *P. berghei* sporozoites of the respective parasite stages using the Advantage RT-PCR kit (Clontech). cDNAs were separated on 1.0% agarose gels and transferred to nylon membranes (Roche Molecular Biochemicals). Gene-specific probes were labeled using digoxigenin-dUTP (Roche Molecular Biochemicals) and hybridized to the cDNA blot. For the dot blot analysis the reverse approach was employed. Representative cDNA inserts obtained from the subtraction screen were PCR amplified with the T7 and M13 reverse primers. Appr. 1 μg of each PCR insert was spotted onto a nylon membrane, denatured and hybridized to digoxigenin-dUTP-labeled cDNA populations from the respective parasite stages. For Western blot analysis, protein extracts from 50,000 sporozoites from either oocysts, hemocoel, or salivary glands were separated on a 10% SDS-PAGE and electrophoretically transferred onto polyvinylidene difluoride membranes. The antibodies to *P. berghei* TRAP and CS have been described previously (3). Bound antibody was detected with horseradish peroxidase-coupled goat anti-rabbit or anti-mouse IgG (Kirkegaard & Perry Laboratories, Gaithersburg, MD), respectively, and developed with enhanced chemiluminescence (ECL; Amersham Biosciences).

Quantitative Real-Time RT-PCR—Two million salivary gland and two million oocyst sporozoites of *P. yoelii* were purified over a DEAE-cellulose column to remove contaminating mosquito tissue. This resulted in 500,000 highly purified parasites for each population. Total RNA was isolated using the RNeasy Mini kit (Qiagen, Valencia, CA). RNA was treated with DNase I (Invitrogen) to remove contaminating genomic DNA. Twenty ng of RNA for each sporozoite population was used as a template in first-strand cDNA synthesis, using the TaqMan® reverse transcriptase kit (PerkinElmer Life Sciences). Gene-specific oligonucleotide primers were designed using the Primer Express software (PerkinElmer Life Sciences). Sequences for oligonucleotides are as follows: (i) *TRAP*, 5′-CATCTGACTCAGAAGTAGAATATCCAAGA-3′ (sense) and 5′-TATGGGTTATCACCTGGTGATGG-3′ (antisense); (ii) *CS,* 5′-AGCCCAAAGAAACTTAAACGAGC-3′ (sense) and 5′-GCCAAGTAATCTGTTGACTATATTTCGA-3′ (antisense); (iii) *UIS1*, 5′-ATTGTCAGTATGAATGATTTTTGGTTAGA-3′ (sense) and 5′-TGTTGTCTTTTTTCACGCCG-3′ (antisense); (iv) *UIS10,* 5′-CACCTGAAGCAGTGGTCGAG-3′ (sense) and 5′-TCAACTGAAGGATCATCTTTATCAGC-3′ (antisense); (v) *UIS16*, 5′-ATCCGACGAAATTCTAGCTATTGAA-3′ (sense) and 5′-GGCCTTAGGATAGATAAAAAGAGCAA-3′ (antisense); and (vi) *UIS24*, 5′-GCATCAAAGCCAAATTTACCAGA-3′ (sense) and 5′-TGTTCTATTACCTTGATCGTTTGCA-3′ (antisense). Amplicon size for all oligonucleotide primer pairs was kept constant at ~ 200 bp. PCR fragments were cloned into plasmid pCR4 (Invitrogen). Each plasmid construct was used in a 10-fold dilution series (10 copies to 10^6 copies, each in triplicate) to determine a standard curve. The standard curve plots the threshold value (*Ct*), defined as the cycle number at which reporter dye fluorescent intensity increases over background, over plasmid copy number. Absolute transcript copy number for each gene is calculated based on the external standard curve. Real-time RT-PCR amplification was done in a GeneAmp® 5700 Sequence detection System (PerkinElmer Life Sciences) using the double-stranded DNA binding probe SYBR Green I® (PerkinElmer Life Sciences). Reactions were subjected to one cycle of 10 min at 95 °C and 45 cycles of 15 s at 95 °C, 1 min at 60 °C. Real-time RT-PCR experiments were done in triplicate.

RESULTS

Constitutive Expression of CS and TRAP in Sporozoites—Differential infectivity of salivary gland and oocyst sporozoites may result from a major difference in expression levels of cell surface ligands. We first asked whether the two characterized sporozoite-specific genes *CS* and *TRAP* are differentially expressed. In order to compare transcript abundance, we generated amplified cDNAs from poly(A)$^+$ RNA of 1 million purified *P. berghei* parasites of either late blood stage schizonts, mature salivary gland sporozoites, or oocyst sporozoites, respectively. Next, we hybridized the stage-specific cDNAs with gene-specific labeled probes (Fig. 2*A*). No significant differences in transcript abundance for either *CS* or *TRAP* were observed between the sporozoite stages. As expected, transcripts of *CS* and *TRAP* were absent in late blood stage schizonts. To control for similar

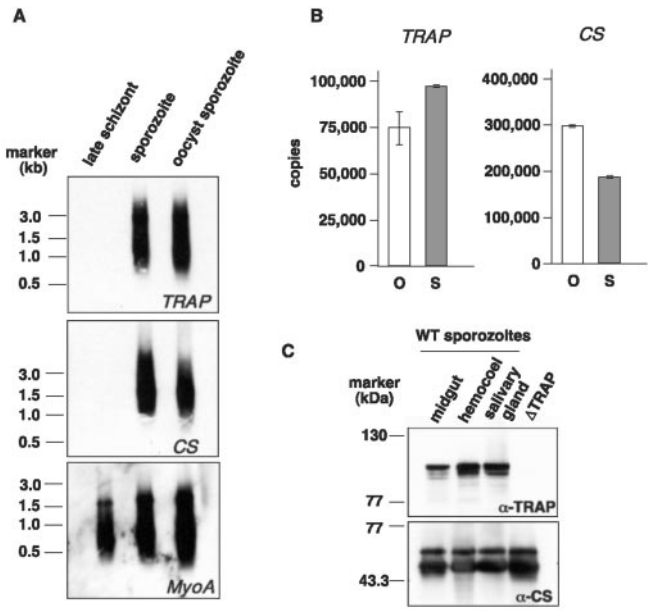

FIG. 2. **Constitutive expression of the sporozoite-specific genes *CS* and *TRAP* throughout sporozoite development.** *A*, cDNA blots of either synchronized late schizonts, salivary gland, or oocyst sporozoites of *P. berghei* hybridized to labeled probes of the genes encoding the sporozoite invasin TRAP or the major surface protein CS. As a control, cDNA blots were hybridized with a probe for the class XIV myosin gene *MyoA*, expressed in all invasive stages. cDNAs were generated from poly(A)$^+$ RNA of 1×10^6 parasites of the respective stage by RT-PCR and amplified once using the SMART (switching mechanism at the 5′ end of RNA transcript) technology. *B*, quantitative real-time RT-PCRs with total RNA from 5×10^5 purified *P. yoelii* sporozoites from either oocysts (*O*) or salivary glands (*S*) as templates using gene-specific oligonucleotide primer pairs to *CS* and *TRAP*. Transcript quantity is represented as the number of copies (± S.D.) in comparison with an external standard curve generated with gene-specific plasmids. Each experiment was done in triplicate. *C*, Western blot analysis. Protein extracts of 50,000 wild-type sporozoites from either oocysts, hemocoel, or salivary glands and 50,000 oocyst sporozoites from *TRAP*(−) parasites were probed with either polyclonal anti-TRAP repeats antiserum or a monoclonal anti-CS antibody. Specificity of the TRAP signal is confirmed by the absence of signal in the *TRAP*(−) sporozoites.

loading we reprobed the same blots with a probe for *MyoA*, a myosin that is expressed in all invasive *Plasmodium* stages (14, 15). In order to independently confirm these results, we employed QRRT-PCR using total RNA of a different rodent malaria parasite, *P. yoelii* (Fig. 2*B*). The results show that transcript levels of the *CS* and *TRAP* genes are similar in oocyst sporozoites and salivary gland sporozoites, confirming the cDNA blot results. We also compared TRAP and CS protein levels during sporozoite maturation (Fig. 2*C*). No dramatic differences were observed, indicating that these gene products are unlikely to determine the profound differences in the phenotype of sporozoites.

Differential Gene Expression in Infectious Plasmodium Sporozoites—To test whether differential gene expression occurs during sporozoite maturation, we wished to compare transcript profiles of infectious salivary gland sporozoites with non-infectious oocyst sporozoites. Sporozoites have to be isolated from infected mosquitoes and are highly contaminated with mosquito tissue. For our experiments, we collected 4 million *P. berghei* sporozoites from the two respective stages in order to obtain 1 million highly purified salivary gland sporozoites and 1 million highly purified oocyst sporozoites. RNA extraction yielded around 50 ng of poly(A)$^+$ RNA for each population that was used as a template for cDNA amplification. For all hybridization experiments throughout this work we used the additional amplification step because several attempts to detect a signal from first-strand cDNA synthesized from 50 ng of poly(A)$^+$ RNA failed.[2] Importantly, the comparison of QRRT-PCR experiments with the cDNA blot analysis for *CS* and *TRAP* (Fig. 2, *A* and *B*) indicated that amplification of cDNAs does not significantly bias gene representation and can be used to compare transcript expression levels of different parasite stages. We could therefore perform a cDNA-based screening technique, suppression subtractive hybridization, with low amounts of starting material. Suppression subtractive hybridization allows selective enrichment of differentially regulated cDNAs of high and low abundance that are present in only one population. This is achieved through a combination of hybridization and PCR amplification protocols that allow simultaneous normalization and subtraction of the cDNA populations (13). We enriched for up-regulated transcripts of *P. berghei* salivary gland sporozoites by using the sporozoite cDNA as our tester cDNA. The driver was a mixture of cDNAs generated from oocyst sporozoites and uninfected salivary glands (to eliminate possible contaminating salivary gland transcripts). Analysis of *P. berghei* cDNA sequences isolated by our subtraction screen was facilitated by the genome sequence data from *P. falciparum* and *P. yoelii* (PlasmoDB.org) as well as *P. berghei* genome sequence data (www.sanger.ac.uk). We sequenced 300 cDNA clones and matched their sequences to the genome sequence data bases. None of the sequenced clones was of mosquito origin. Cluster analysis revealed 32 individual genome contigs that were tagged by at least 2 sequenced cDNA clones. Notably, we did not isolate any of the genes that are expressed throughout *Plasmodium* sporozoite maturation, *i.e.* *MyoA*, *CS*, and *TRAP*.

To further select only those genes that are specifically up-regulated in salivary gland sporozoites, we probed dot-blots of representative cDNAs for each genome contig with labeled amplified total cDNA probes from different stages of the *Plasmodium* life cycle (Fig. 3). Among the 32 genes recovered, 2 genes (A2 and F4) were abundantly transcribed in all stages tested by dot-blot analysis, thereby identifying them as false positives that could serve as independent internal controls. F4 encodes the *P. berghei* ortholog of the large subunit of RNA polymerase I of *P. falciparum* (16), a likely constitutive protein required for rRNA synthesis throughout the *Plasmodium* life cycle. No function could be assigned to clone A2.

The dot-blot analysis demonstrates that the remaining 30 genes are up-regulated in infective sporozoites isolated from the mosquito salivary glands (termed *UIS* genes). We conclude that maturation of infectivity in *Plasmodium* sporozoites is accompanied by dramatic changes in their transcriptional repertoire.

MCP-1 Is Expressed in Two Invasive Plasmodium Stages—One gene (*UIS16*) displayed a unique expression pattern. It is enriched both in salivary gland sporozoites and blood stage schizonts (clone E3 in Fig. 3). *UIS16* encodes the *P. berghei* ortholog of the previously described *P. falciparum* MCP-1. MCP-1 is expressed in invasive merozoites and appears to be located initially at the attachment site between merozoites and erythrocytes, and then it migrates backwards around the merozoites during invasion of the red blood cells (17, 18). Invasion proceeds by a "moving junction" between the membrane of the parasite and the membrane of the host cell. It has been proposed that MCP-1 participates in the movement of the junction along the parasite's cytoskeleton (17). Our findings suggest that MCP-1 has a similar function during invasion of red blood cells by merozoites and invasion of hepatocytes by salivary gland sporozoites.

[2] K. Matuschewski, J. Ross, S. M. Brown, K. Kaiser, V. Nussenzweig, and S. H. I. Kappe, unpublished results.

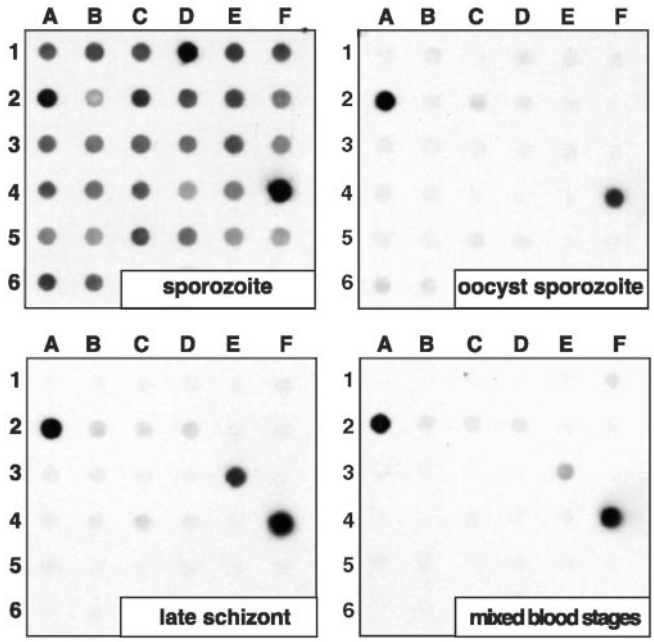

FIG. 3. **Identification of *Plasmodium UIS* genes.** Thirty-two genes were redundantly recovered in a suppression subtractive hybridization screen designed to enrich salivary gland sporozoite-specific transcripts and further tested for differential expression. Dot-blots of the cDNA inserts were hybridized with labeled total cDNA probes generated from salivary gland or oocyst sporozoites as well as synchronized late blood stage schizonts and mixed blood stages that contain all erythrocytic asexual and sexual forms of the malaria parasite. Two clones (A2 and F4) are false positives and serve as independent internal controls. *UIS16* (clone E3) encodes a protein previously described as MCP-1. Note the up-regulation of *MCP-1* during sporozoite maturation as well as enrichment in the late schizont stage. The remaining 29 genes are highly up-regulated in virulent salivary gland sporozoites. They are not expressed at significant levels in the parasites blood stages.

Genes That Are Specifically Up-regulated in Infective Sporozoites—Remarkably, the 29 remaining *UIS* genes are not expressed at significant levels in the parasite blood stages (Fig. 3). Schematic diagrams of the deduced proteins for each *UIS* are presented in Fig. 4. Overall, we identified novel stage-specific genes that encode putative-regulatory proteins, such as kinases and phosphatases as well as transcriptional regulators. Other UIS gene products have predicted enzymatic activities. In addition, a number of predicted proteins display consensus amino-terminal signal peptides and/or internal hydrophobic segments that could function as transmembrane domains.

The most frequently recovered gene (*UIS1*, 26% of all sequences) encodes a protein kinase. UIS1 contains the conserved kinase motifs but could not be classified into one specific kinase subfamily. A number of putative secreted molecules are differentially expressed in salivary gland sporozoites. For example, *UIS2* (7% of all sequences) encodes a secreted molecule with a region of homology to purple acid phosphatases. *In vitro*, these enzymes resemble phosphomonoesterases; however, their physiological function remains to be established.

In order to validate our findings, we performed independent expression experiments for selected *UIS* genes (Fig. 5). To demonstrate that PCR amplification of transcripts had not biased representation, we compared the cDNA blot methodology with expression data generated by QRRT-PCR. A blot of amplified cDNA of oocyst sporozoites, salivary gland sporozoites, and late blood stage schizonts hybridized with a *UIS1* probe detected no transcripts in *P. berghei* oocyst sporozoites or blood stage schizonts, whereas transcripts were abundant in salivary gland sporozoites (Fig. 5*A*). QRRT-PCR data generated separately from *P. yoelii* sporozoites showed an ~24-fold up-regulation of *UIS1* transcripts in salivary gland sporozoites when compared with oocyst sporozoites (Fig. 5*A*), confirming differential expression of *UIS1* during sporozoite maturation. Transcript abundance for *UIS10* encoding a lecithin-cholesterol acyltransferase was up-regulated ~16-fold during sporozoite maturation (Fig. 5*B*).

Although subtractive hybridization screens are not exhaustive, and other *UIS* genes may be identified in the future through additional approaches, we most likely identified a significant portion of genes that are up-regulated during sporozoite maturation. As shown in Fig. 4, *UIS1* to *UIS13* were recovered frequently in our screen. In good agreement with these data, we observed strong differential expression by either cDNA blot analysis or QRRT-PCR or both[2] for *UIS3* and *UIS4*, both of which encode small molecules containing potential transmembrane domains, and *UIS5*, which encodes a putative aminotransferase class V.

To test whether up-regulation of transcript abundance is still significant for *UIS* genes recovered only twice in our subtraction screen, we performed QRRT-PCR experiments for two representative genes (Fig. 5*B*). Transcript abundance increased ~8-fold for *UIS16*/*MCP1* and ~6-fold for *UIS24*/*HSP70–3* in salivary gland sporozoites compared with oocyst sporozoites.

DISCUSSION

In this study, we identify the first candidate infectivity genes of *Plasmodium* sporozoites. We demonstrate that the sporozoites located in the salivary glands differ significantly in their transcriptional repertoire from sporozoites emerging from oocysts. These findings, taken together with the dramatic phenotypic differences (7–10), show that maturation of *Plasmodium* sporozoite infectivity for the mammalian host follows a developmental program. We found that salivary gland sporozoites up-regulate many genes that are not expressed earlier in development. Among them are potential regulatory proteins, secretory molecules, and metabolic enzymes that probably control sporozoite virulence. Sporozoites residing in the salivary gland are programmed to invade hepatocytes and to continue the life cycle in the mammalian host. The associated phenotypical and molecular changes are probably irreversible because salivary gland sporozoites introduced into the hemocoel of mosquitoes are no longer capable of reentering the salivary glands (11).

Sporozoite transmission during the mosquito bite is one of the bottlenecks in the *Plasmodium* life cycle (19). A sporozoite within the mosquito salivary gland has to reach the mammalian liver, invade a suitable hepatocyte, and commence development into an EEF. Some of the *UIS* genes most likely participate in these events. Support for this comes from our finding that *UIS16* encodes MCP-1, the only UIS protein characterized previously in invading merozoites. MCP-1/UIS16 localized to the moving junction between merozoites and host red blood cell, leading to the formation of a parasitophorous vacuole (17). MCP-1 expression was tightly regulated. It was only seen in merozoites but not in earlier blood stages. It is likely that MCP-1 performs a similar function in the merozoite and the salivary gland sporozoite. The presence of *MCP-1* in the subtraction screen provides support for the identification of genes that control parasite infectivity using differential gene expression profiling.

The noise in our screen is remarkably low. Among 32 selected candidates, we obtained only 2 false positives (A2 and F4 in Fig. 3). We believe that mainly two factors contributed to the success: (i) the purity of the starting material as well as mixing uninfected mosquito material to the driver population, and (ii)

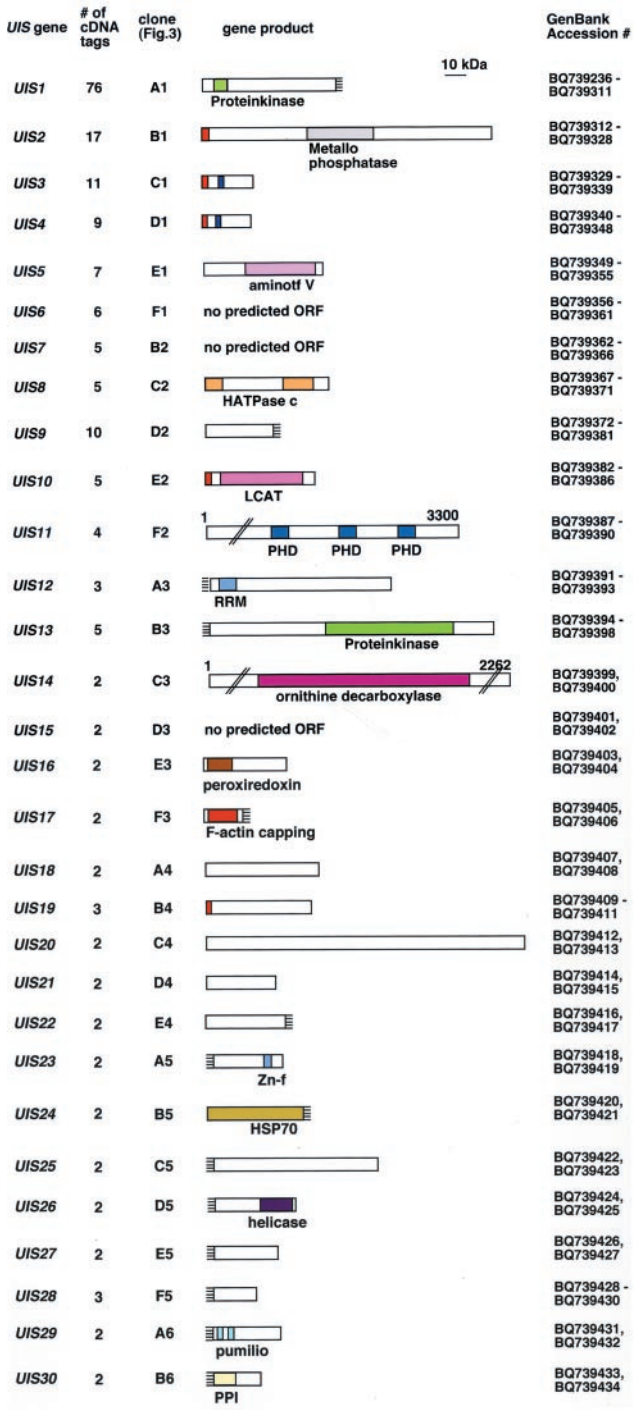

FIG. 4. **Schematic diagrams of the predicted primary structure of the *P. yoelii* gene products encoded by *UIS*.** Putative cleavable signal peptides are indicated by *red boxes*, and putative transmembrane domains are shown as *blue boxes*. Putative protein domains with assigned functions are represented by *different-colored boxes*. For each *UIS* gene, the number of clones identified in the suppression subtractive hybridization screen and the respective GenBank™ accession numbers for cDNA clones are shown. Note that for a number of *UIS* genes, ORFs are truncated due to the incompleteness of the corresponding genomic contigs. No ORFs are predicted for *UIS6*, *UIS7*, and *UIS15*. *aminotf V*, aminotransferase class V; *HATPase c*, histidin ATPase c; *LCAT*, lecithin-cholesterol acyltransferase; *PHD*, (plant homeo domain) finger motif; *PPI*, peptidyl prolyl cis/trans isomerase; *RRM*, RNA recognition motif; *Zn-f*, zinc finger.

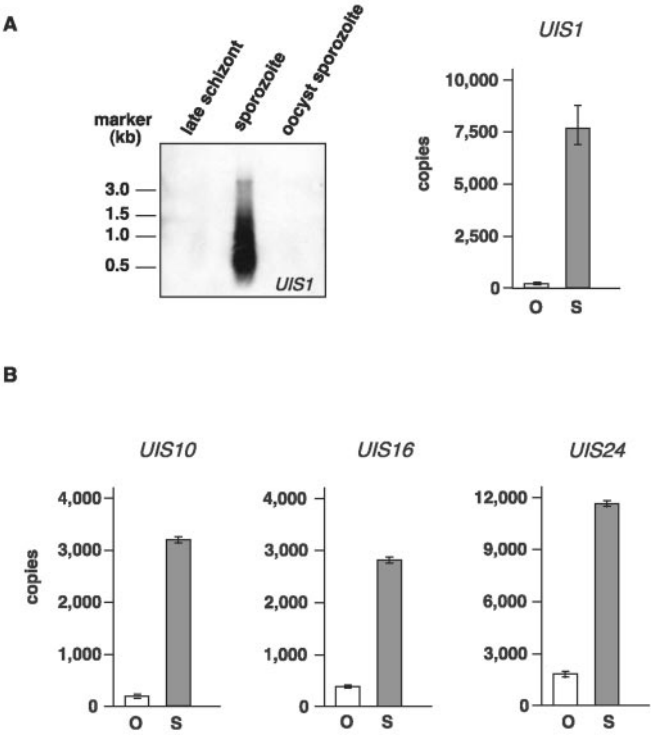

FIG. 5. **Stage-specific up-regulation of selected *UIS* genes is confirmed by QRRT-PCR.** *A,* comparison of expression analysis of *UIS1* by blot of amplified cDNA (*P. berghei*) and QRRT-PCR (*P. yoelii*). Both experiments confirm that *UIS1* transcript abundance increases dramatically in salivary gland sporozoites (*S*) when compared with oocyst sporozoites (*O*). No expression of *UIS1* can be detected in late blood stage schizonts by cDNA blot. Compare restriction of transcript expression with the constitutive sporozoite-specific genes *TRAP* and *CS* (Fig. 2, *A* and *B*). *B,* QRRT-PCR analysis of *P. yoelii* transcript abundance for additional *UIS* in oocyst (*O*) and salivary gland (*S*) sporozoites confirms differential *UIS* expression. Shown are the transcript levels of *P. yoelii LCAT*/*UIS10*, *MCP1*/*UIS16,* and *HSP70–3*/*UIS24*. Transcript quantity is represented as the number of copies (±S.D.) in comparison with an external standard curve generated with gene-specific plasmids. Each experiment was done in triplicate.

the threshold of at least two hits. Based on the significant up-regulation of *UIS* genes that just met the threshold level (Fig. 5*B*), we may recover additional candidate genes that are developmentally regulated among the single-hit cDNAs.

Regulation of gene expression is probably the major mechanism that underlies the development of sporozoite infectivity. MCP-1 and other UIS proteins may be involved in salivary gland sporozoite invasion of target cells. Others could be important in adapting to new metabolic requirements within the infected hepatocyte. *UIS10* is an example of a secretory molecule that is likely to function during EEF replication. It encodes lecithin-cholesterol acyltransferase. Lecithin-cholesterol acyltransferase (20) is the major cholesterol esterifying activity in human plasma, and in addition it facilitates reverse cholesterol transport. The mevalonate pathway of sterol biosynthesis has not been identified in *Plasmodium*. Therefore, the parasite's cholesterol is most likely host-derived. The *Plasmodium* EEFs have a very high demand for membrane biogenesis because they generate thousands of merozoites. Thus, UIS10 may participate in the transport of cholesterol from the hepatocyte into EEFs. UIS10 contains the signature sequence GXSXG that is conserved in the active site of lipases, as well as the loop region that confers binding of lecithin-cholesterol acyltransferase to the surface of lipoproteins (20). In the related apicomplexan parasite *Toxoplasma gondii*, the mobilization of cholesterol from host cell lysosomes is required for intracellular growth (21), but the underlying enzymatic mechanisms that allow the parasite to utilize an exogenous supply of cholesterol have not been identified. In accordance with a function in EEF, we can detect lecithin-cholesterol acyltransferase transcripts 20 h (at

this time point, all invaded sporozoites have transformed into EEFs) after sporozoite invasion of cultured hepatoma cells.[2] *UIS14* is a member of the ornithine/methionine decarboxylase family. These enzymes participate in the initial steps in the synthesis of polyamines, molecules that are crucial for cell differentiation and proliferation in animals, plants, and bacteria (22). *UIS14* differs substantially from the *P. falciparum* bifunctional ornithine, *S*-adenosylmethionine decarboxylase (*ODC/AdoMetDC*) (23). UIS14 is strikingly similar to the bacterial enzymes, in particular to *Mycobacterium* ornithine decarboxylase, but differs greatly in amino acid sequence from the eukaryotic enzymes. Earlier studies indicated that difluoromethylornithine, an enzyme-activated irreversible inhibitor of ornithine decarboxylase, inhibited liver stage schizogony but had little or no effect on the erythrocytic schizogony *in vivo* (24, 25). These observations were previously explained by the different pharmacokinetics of difluoromethylornithine in red cells and in hepatocytes. Our findings suggest instead that ornithine decarboxylase performs a vital function in the pre-erythrocytic stages (most likely during DNA replication in EEFs) and that the polyamine requirements are differentially regulated in blood stages and EEFs.

UIS genes may encode key regulators themselves. For example, *UIS1* encodes a novel protein kinase. Although the function of *UIS1* and its product remains to be elucidated by reverse genetics and biochemical approaches, it could participate in the signaling events associated with gliding motility, hepatocyte invasion, and/or the transformation of sporozoites into EEFs.

What are the signals that induce *UIS* transcript up-regulation? One possibility is that *Plasmodium* sporozoites undergo a time-dependent endogenous developmental program. Thus, independently of external signals, sporozoites gradually increase expression of *UIS*, and completion of maturation coincides with their entry into the salivary glands. This hypothesis could be tested in the recently developed culture system for *P. berghei* oocysts (26) that leads to the production of sporozoites that are infective for mice. However, the *in vitro*-produced sporozoites are ~1,000-fold less infective for rodents when compared with the levels of salivary gland sporozoite infectivity (3, 10). Therefore, the increase in infectivity could be associated with an outside signal that coincides with sporozoite entry of mosquito salivary glands. Recent studies suggest that *Plasmodium* sporozoites may indeed selectively recognize specific receptors on salivary glands (27–29). Perhaps sporozoite interactions with putative salivary gland receptors trigger the onset of a new gene expression program.

Because transcription of most *UIS* genes is restricted to salivary gland sporozoites, they can be targeted by reverse genetics. This should reveal those gene products that perform crucial functions for the sporozoite's successful journey from the mosquito salivary gland into hepatocytes and for its subsequent development into EEFs. Functional complementation of *uis*-null mutants with the corresponding *P. falciparum* sequences will ultimately prove whether the *UIS* genes identified in this study are true functional orthologs of the human malaria parasite.

The developmentally up-regulated genes identified in this study are important stepping stones for the dissection of the molecular mechanism underlying sporozoite maturation and, as a consequence, infectivity to the mammalian host. *UIS* genes can serve as a gateway for the identification of parasite genes expressed in the EEF. In fact, we have performed RT-PCR with *UIS*-specific oligonucleotide primers using RNA isolated from HepG2 cells 20 h after infection with *P. berghei* sporozoites. Of seven *UIS* genes tested, six are expressed in EEF at this time point.[2]

Acknowledgments—We thank Ivette Caro-Aguilar for expert technical assistance and Oscar Bruna-Romero for the introduction to the QRRT-PCR techniques. Preliminary sequence and/or preliminary annotated sequence data from the *P. yoelii* genome was obtained from The Institute for Genomic Research website (www.tigr.org). This sequencing program is carried on in collaboration with the Naval Medical Research Center and is supported by the United States Department of Defense. We thank the scientists and funding agencies comprising the international Malaria Genome Project for making sequence data from the genome of *P. falciparum* (3D7) public prior to publication of the completed sequence. The Sanger Centre (United Kingdom) provided sequence for chromosomes 1, 3–9, and 13, with financial support from the Wellcome Trust. A consortium composed of The Institute for Genome Research, along with the Naval Medical Research Center, sequenced chromosomes 2, 10, 11, and 14, with support from National Institute of Allergy and Infectious Diseases/National Institutes of Health, the Burroughs Wellcome Fund, and the Department of Defense. The Stanford Genome Technology Center sequenced chromosome 12, with support from the Burroughs Wellcome Fund. The *Plasmodium* Genome Data base is a collaborative effort of investigators at the University of Pennsylvania and Monash University (Melbourne, Australia), supported by the Burroughs Wellcome Fund.

REFERENCES

1. Aikawa, M., Yoshida, N., Nussenzweig, R. S., and Nussenzweig, V. (1981) *J. Immunol.* **126,** 2494–2495
2. Menard, R., Sultan, A. A., Cortes, C., Altszuler, R., van Dijk, M. R., Janse, C. J., Waters, A. P., Nussenzweig, R. S., and Nussenzweig, V. (1997) *Nature* **385,** 336–340
3. Sultan, A. A., Thathy, V., Frevert, U., Robson, K. J., Crisanti, A., Nussenzweig, V., Nussenzweig, R. S., and Menard, R. (1997) *Cell* **90,** 511–522
4. Matuschewski, K., Nunes, A. C., Nussenzweig, V., and Menard, R. (2002) *EMBO J.* **21,** 1597–1606
5. Tsuji, M., Rodrigues, E. G., and Nussenzweig, R. S. (2001) *Biol. Chem.* **382,** 553–570
6. Miller, L. H., and Hoffman, S. L. (1998) *Nat. Med.* **4,** 520–524
7. Nussenzweig, R. S., Vanderberg, J. P., Most, H., and Orton, C. (1969) *Nature* **222,** 488–489
8. Vanderberg, J. P., Nussenzweig, R. S., Sanabria, Y., Nawrot, R., and Most, H. (1972) *Proc. Helminth. Soc. Wash.* **39,** 514–525
9. Vanderberg, J. P. (1974) *J. Protozool.* **21,** 527–537
10. Vanderberg, J. P. (1975) *J. Parasitol.* **61,** 43–50
11. Touray, M. G., Warburg, A., Laughinghouse, A., Krettli, A. U., and Miller, L. H. (1992) *J. Exp. Med.* **175,** 1607–1612
12. Kappe, S. H., Gardner, M. J., Brown, S. M., Ross, J., Matuschewski, K., Ribeiro, J. M., Adams, J. H., Quackenbush, J., Cho, J., Carucci, D. J., Hoffman, S. L., and Nussenzweig, V. (2001) *Proc. Natl. Acad. Sci. U. S. A.* **98,** 9895–9900
13. Diatchenko, L., Lau, Y. F., Campbell, A. P., Chenchik, A., Moqadam, F., Huang, B., Lukyanov, S., Lukyanov, K., Gurskaya, N., Sverdlov, E. D., and Siebert, P. D. (1996) *Proc. Natl. Acad. Sci. U. S. A.* **93,** 6025–6030
14. Pinder, J. C., Fowler, R. E., Dluzewski, A. R., Bannister, L. H., Lavin, F. M., Mitchell, G. H., Wilson, R. J., and Gratzer, W. B. (1998) *J. Cell Sci.* **111,** 1831–1839
15. Matuschewski, K., Mota, M. M., Pinder, J. C., Nussenzweig, V., and Kappe, S. H. (2001) *Mol. Biochem. Parasitol.* **112,** 157–161
16. Fox, B. A., Li, W. B., Tanaka, M., Inselburg, J., and Bzik, D. J. (1993) *Mol. Biochem. Parasitol.* **61,** 37–48
17. Klotz, F. W., Hadley, T. J., Aikawa, M., Leech, J., Howard, R. J., and Miller, L. H. (1989) *Mol. Biochem. Parasitol.* **36,** 177–185
18. Hudson-Taylor, D. E., Dolan, S. A., Klotz, F. W., Fujioka, H., Aikawa, M., Koonin, E. V., and Miller, L. H. (1995) *Mol. Microbiol.* **15,** 463–471
19. Ghosh, A., Edwards, M. J., and Jacobs-Lorena, M. (2000) *Parasitol. Today* **16,** 196–201
20. Jonas, A. (2000) *Biochim. Biophys. Acta* **1529,** 245–256
21. Coppens, I., Sinai, A. P., and Joiner, K. A. (2000) *J. Cell Biol.* **149,** 167–180
22. Tabor, C. W., and Tabor, H. (1984) *Annu. Rev. Biochem.* **53,** 749–790
23. Müller, S., Da'dara, A., Luersen, K., Wrenger, C., Das Gupta, R., Madhubala, R., and Walter, R. D. (2000) *J. Biol. Chem.* **275,** 8097–8102
24. Hollingdale, M. R., McCann, P. P., and Sjoerdsma, A. (1985) *Exp. Parasitol.* **60,** 111–117
25. Francois, G., Van Looveren, M., and Timperman, G. (1997) *Ann. Trop. Med. Parasitol.* **91,** 103–106
26. Al-Olayan, E. M., Beetsma, A. L., Butcher, G. A., Sinden, R. E., and Hurd, H. (2002) *Science* **295,** 677–679
27. Barreau, C., Touray, M., Pimenta, P. F., Miller, L. H., and Vernick, K. D. (1995) *Exp. Parasitol.* **81,** 332–343
28. Brennan, J. D., Kent, M., Dhar, R., Fujioka, H., and Kumar, N. (2000) *Proc. Natl. Acad. Sci. U. S. A.* **97,** 13859–13864
29. Ghosh, A. K., Ribolla, P. E., and Jacobs-Lorena, M. (2001) *Proc. Natl. Acad. Sci. U. S. A.* **98,** 13278–13281
30. Natarajan, R., Thathy, V., Mota, M. M., Hafalla, J. C., Menard, R., and Vernick, K. D. (2001) *Cell. Microbiol.* **3,** 371–379

MOLECULAR BASIS OF CELL AND DEVELOPMENTAL BIOLOGY:

Infectivity-associated Changes in the Transcriptional Repertoire of the Malaria Parasite Sporozoite Stage

Kai Matuschewski, Jessica Ross, Stuart M. Brown, Karine Kaiser, Victor Nussenzweig and Stefan H. I. Kappe

J. Biol. Chem. 2002, 277:41948-41953.
doi: 10.1074/jbc.M207315200 originally published online August 12, 2002